JOURNAL OF VIROLOGY, Dec. 1999, p. 10447–10457 Vol. 73, No. 12
0022-538X/99/$04.00+0

Vesicular Stomatitis Virus G Protein Acquires pH-Independent Fusion Activity during Transport in a Polarized Endometrial Cell Line

PAUL C. ROBERTS,* TODD KIPPERMAN, AND RICHARD W. COMPANS

Department of Microbiology and Immunology, Emory University School of Medicine, Atlanta, Georgia 30322

Received 28 May 1999/Accepted 19 August 1999

Entry of vesicular stomatitis virus (VSV), the prototype member of the rhabdovirus family, occurs by receptor-mediated endocytosis. Subsequently, during traversal through the endosomal compartments, the VSV G protein acquires a low-pH-induced fusion-competent form, allowing for fusion of the viral membrane with endosomal and lysosomal membranes. This fusion event releases genomic RNA into the cytoplasm of the cell. Here we provide evidence that the VSV G protein acquires a fusion-competent form during exocytosis in a polarized endometrial cell line, HEC-1A. VSV infection of HEC-1A cells results in high viral yields and giant cell formation. Syncytium formation is blocked in a concentration-dependent manner by treatment with the lysosomotropic weak base ammonium chloride, which raises intravesicular pH. Virus release is somewhat delayed by treatment with ammonium chloride, but virus yields gradually reach those of control cells. In addition, inhibition of vacuolar H^+-ATPases by treatment with bafilomycin A1 also inhibited cell to cell fusion without altering virus yields. Virions released from infected HEC cells were themselves not fusion competent, since viral entry required an active H^+-ATPase and a low-pH-induced conformational change in the viral G protein. Thus, the conformation change leading to fusion competence during exocytotic transport is reversible and reverts during or after release of the virion from the infected cell.

Enveloped viruses initiate infection by membrane fusion between viral and host cell membranes. In general, enveloped viruses employ one of two alternative mechanisms to initiate viral-host cell membrane fusion, a process which is mediated by the viral fusion protein. Viruses belonging to the *Retroviridae*, *Paramyxoviridae*, *Herpesviridae*, and *Coronaviridae* families typically initiate fusion in a pH-independent manner (26) whereby the virion initially binds to cell surface receptors and subsequently the viral membrane fuses with the plasma membrane of the host cell at neutral pH. The second, more complex route of entry is characterized by cell surface binding of the virion, followed by endocytosis and transport to the endosomal and lysosomal compartments, where the viral fusion proteins are activated by exposure to the low pH milieu of these compartments. Thus, the latter route is referred to a low-pH-dependent fusion. Presumably, the low pH of endosomal and lysosomal compartments is regulated by the action of vacuolar H^+-ATPases, which function also to create an active H^+ gradient which maintains membrane potential (31). Viruses belonging to the *Orthomyxoviridae*, *Togaviridae*, *Rhabdoviridae*, *Bunyaviridae*, and *Arenaviridae* families typically require a low-pH-mediated event for efficient fusion of viral and host cellular membranes (26).

Vesicular stomatitis virus (VSV), the prototype member of the *Rhabdoviridae*, is a bullet-shaped, enveloped virus containing a single-stranded RNA genome of negative polarity which encodes five viral proteins. There is only one viral glycoprotein present in the virion membrane, the G protein, which functions as the virus attachment and fusion protein. The G protein is a transmembrane protein containing two N-linked glycans (9). In the absence of other viral proteins, the G protein can initiate membrane fusion in a low-pH-dependent manner (17, 42). VSV G protein-mediated fusion is readily inhibited by treatment with lysosomotropic agents, such as chloroquine and ammonium chloride (14, 43, 48). Presumably, low-pH exposure triggers a conformational change in the G protein allowing it to induce membrane fusion either between viral and host cell membranes or between infected cells expressing the viral G protein at the cell surface. In the latter case, brief exposure of infected cells to low pH results in the formation of multinucleated polykaryons, which can be easily quantitated (4, 32, 41). The VSV G protein does not reach the cell surface in a fusion-competent form during the usual replication cycle. Thus, polykaryon formation is not a normal cytopathic effect in the life cycle of the rhadoviruses.

Most viral fusion proteins contain a fusion peptide that is largely hydrophobic, which upon exposure to membranes can mediate membrane fusion either in a low-pH-dependent or pH-independent manner (26). In the case of the VSV G protein, the fusion peptide appears to reside at an internal location of the protein between amino acids 117 and 137 and is comprised of neutral amino acids (16, 18, 29, 57, 59). In addition to the requirement for an internal fusion peptide, the viral G protein also requires some form of membrane anchoring in order to promote membrane fusion (36). More recently, it was found that conserved glycine residues within the transmembrane domain of the viral G protein appear to be required for fusion activity (8). Other regions distal to the internal fusion peptide that can influence fusion activity have been identified, suggesting that the conformation of the fusion peptide is regulated by the three-dimensional structure of the G protein obtained after low-pH exposure (50, 51). Interestingly, studies with rabies virus G protein have shown that the G protein can undergo several conformational changes that are pH dependent and can influence fusion activity (20, 21, 23). The rabies virus G protein is thought to be transported initially in an inactive state during intracellular transport to avoid fusion in the acidic Golgi vesicles and subsequently acquires its native state at or near the cell surface (23). These transitional states have also been postulated to occur with the VSV G protein, based on kinetic studies (7, 40). However, it is unclear whether

* Corresponding author. Present address: Department of Immunology and Microbiology, Wayne State University School of Medicine, Detroit, MI 48201. Phone: (313) 577-6494. Fax: (313) 577-1155. E-mail: proberts@med.wayne.edu.

a similar inactive state is a transport intermediate during VSV G transport.

In the present study, we report the ability of VSV to induce giant cell formation in cell monolayers without prior exposure to extracellular low-pH media. The human endometrial cell line HEC-1A forms an epithelial monolayer that supports entry and release of divergent viruses at distinct plasma membrane domains (3). Thus, this cell line provides a highly polarized environment in which to examine the mechanisms of viral glycoprotein sorting and of virus maturation. The results presented here suggest that in the HEC cell line the viral G protein undergoes a conformational change during intracellular transport allowing for fusion of viral infected cells with surrounding cells in culture, also referred to as induction of fusion from within. These results have interesting implications for transitional states of viral fusion peptides as well as for mechanisms of viral pathogenesis.

MATERIALS AND METHODS

Cells. The HEC-1A cell line (ATCC HTB 112) and the human lung-derived cell line A549 (ATCC CCL 185) were grown and maintained in RPMI 1640 medium supplemented with 10% fetal bovine serum (FBS). Madin-Darby canine kidney (MDCK), human cervical tissue-derived (HeLa), and monkey kidney-derived (Vero C1008) cell lines were propagated in Dulbecco's modified Eagle's medium (DMEM) supplemented with 10% FBS. Baby hamster kidney (BHK-21) cells were grown in DMEM supplemented with 10% FBS and 5% tryptose phosphate broth.

Subclones of the parental HEC-1A cell line were obtained by standard limited dilution and cloning chamber methodologies. Briefly, cells were plated at low density (50 cells per 100-mm-diameter dish) such that single well-isolated colonies of cells would arise from single cells. Isolated colonies were collected by cloning chambers and propagated in RPMI medium. Subcloned cell lines were further evaluated for the ability to establish transepithelial resistance upon seeding on permeable membrane supports as previously described (3). The HECA2 cell line was found to exhibit high transepithelial resistance (1200 ohms/cm^2) and was fully permissive to influenza A virus and VSV infections.

Viruses. The Indiana strain of VSV (VSV_{IND}) was propagated and titered by plaque assay in BHK-21 cells as described previously (3). This strain has undergone multiple laboratory passages. Several isolates of VSV with known passage history were generously provided by Stuart Nichol at the Centers for Disease Control and Prevention, Atlanta, Ga.: $VSV_{NJ/CA}$, (New Jersey strain, California isolate, passage 2), $VSV_{NJ86CRB2}$ (New Jersey strain, Costa Rica isolate, passage 2), VSV_{IND} (isolate L27486, passage 1), and VSV_{IND} (isolate 8687, passage 2). These isolates were propagated one time in BHK-21 cells, and the supernatants were stored frozen at −70°C and used as stock virus.

Virus infections and drug treatments. HEC cells were seeded in 12-well culture dishes (Falcon) and infected at a multiplicity of infection (MOI) of 2. Following a 1-h incubation at 37°C, the cells were washed twice to remove unadsorbed virus, and the infection was continued at 37°C in the presence of RPMI supplemented with 2.5% FBS. At different time points, aliquots of supernatants from infected cells were collected, precleared at 500 × *g* to remove cellular debris, and stored at −70°C until titration by plaque assay. Briefly, BHK-21 cells were infected with serial 10-fold dilutions of virus suspensions. Following a 1-h adsorption period, cells were overlaid with a solution of 0.9% agar in DMEM supplemented with 2.5% FBS. The cells were then incubated at 37°C for 24 to 48 h, at which time the cells were overlaid with an additional agar layer containing neutral red (0.025%). Plaques were visually counted approximately 4 h after the addition of neutral red overlay. Virus yields were expressed as PFU per cell.

In experiments examining the effects of drug treatment on giant cell formation, infected cells were treated with ammonium chloride (2 M stock NH_4Cl prepared in distilled H_2O) or bafilomycin (Bfm) A1 (prepared as a 32 μM stock in dimethyl sulfoxide; Sigma) beginning at 3.5 h postinfection (hpi) so that early virus entry and replication events would not be impaired. In some experiments, the effects of drug treatment on early virus entry mechanisms was determined; here, drug treatment was performed 1 h prior to infection and continued throughout the infection period.

To monitor pH differences during infections, we used ColorpHast pH indicator strips (EM Science, Gibbstown, N.J.), which according to the manufacturers have an accuracy of 0.2 to 0.3 pH units. We also periodically checked the accuracy of these pH strips with known pH buffers. Briefly, at different time points following infection, 100-μl aliquots were removed and immediately monitored for pH with the indicator strips. In addition, we also directly measured the pH of the incubation media (ca. 2 ml) at different time points during infection with a standard pH meter (model 8005; VWR Scientific).

Morphological assessment of virus cytopathogenicity. At different times postinfection, virus-infected monolayers were washed in Hanks' balanced salt solution, fixed for 5 min in 100% methanol, and allowed to air dry. Cells were subsequently stained with Giemsa stain according to the manufacturer's protocol. Monolayers were photographed with a Nikon Diaphot inverted microscope equipped with epifluorescence.

Quantitation of virus fusion. To quantitate viral fusion, nuclei were stained with the nuclear stain 4′,6-diamidino-2-phenylindole (DAPI; Molecular Probes, Eugene, Oreg.) and visualized by using a filter designed for UV fluorescence. Both the number of giant cells (syncytia) and the number of single nuclei were counted in random fields at 20×. The average number of nuclei present per synctia was determined by subtracting the mean number of single nuclei of infected monolayers (not associated with syncytia) from the mean number of single nuclei determined for mock-infected monolayers and then dividing by the mean number of syncytia. The fusion index is thus a measure of the percentage of cells undergoing fusion.

To monitor viral G protein cell surface expression in drug-treated cells, infected cells were briefly exposed to pH 5.7 or 7.2 morpholine-ethanesulfonic acid (MES) buffer (20 mM MES in phosphate-buffered saline [PBS], pH adjusted with HCl or NaOH). Uninfected cells were used as control cells for fusion assays.

Immunofluorescence microscopy. Cell surface expression of the viral G protein was monitored by immunofluorescence staining of infected cell monolayers. Briefly, at different times postinfection, cells grown on glass coverslips were fixed in 3% paraformaldehyde. Surface expression was detected by sequential incubations of fixed cells with mouse monoclonal anti-G antibody (1) followed by Alexa Fluor 488 (Molecular Probes)-conjugated goat anti-mouse immunoglobulin. Fluorescence was monitored and photographed with a Nikon TMD microscope equipped with epifluorescence and a 35-mm camera. In some instances, the organization of the actin microfilament network was monitored. Here, following cell surface staining for VSV G protein, cells were permeablized with Triton X-100 (15 min; 0.2% Triton X-100 in PBS). Actin was visualized by staining cells with tetramethylrhodamine isothiocyanate-conjugated phalloidin (0.6 μg/ml; Sigma). Nuclei were counterstained with the nuclear stain DAPI (Molecular Probes).

^{35}S metabolic labeling of virions. Virus-infected cells (MOI = 5) were incubated in Eagle's medium deficient in methionine and cysteine for 15 min prior to labeling. The cells were subsequently labeled at different time points for 20 min at 37°C with 60 μCi of ^{35}S cell labeling mix (ICN, Dupont). Following labeling, monolayers were washed twice with PBS and lysed in 200 μl of lysis buffer containing 1% Triton X-100 and 0.5% sodium deoxycholate in MNT (20 mM MES [Sigma], 100 mM NaCl, 30 mM Tris-HCl [pH 8.0])–1 mM EDTA–1 mM phenylmethylsulfonyl fluoride.

For ^{35}S labeling of virions, cells were incubated with 60 μCi of ^{35}S cell labeling mix from 5 to 20 hpi. Virions released into the media were precleared of cellular debris by centrifugation at 500 × *g* for 10 min and subsequently pelleted by ultracentrifugation at 20,000 rpm for 1 h at 4°C, using an SW55Ti rotor. Virions were resuspended in equal amounts of Laemmli lysis buffer (28) and stored at −70°C. Aliquots of cell extracts or virions were analyzed by sodium dodecyl sulfate–10% polyacrylamide gel electrophoresis (SDS-PAGE) and fluorography.

Cell-cell fusion assay. HECA2 cells were seeded at low density and infected with VSV at an MOI of 2 under subconfluent conditions. For analysis of virus-infected cell fusion with uninfected target cells, target cells were prelabeled with the lipophilic fluorochrome CellTracker CM-DiI (chloromethylbenzamido-dioctadecyl indocarbocyanine) according to the protocol of the manufacturer (Molecular Probes). Briefly, cell were incubated in PBS containing 1 μg of CM-DiI per ml for 10 min at 37°C and then incubated for 10 min at 4°C. Cell monolayers were washed extensively to remove unincorporated dye and incubated for an additional 1 h at 37°C in normal growth medium. Target cells were subsequently trypsinized and added to infected monolayers at a 1:1 target-to-infected cell ratio. To distinguish between infected and uninfected cells, infected cells were labeled with the fluorochrome probe CellTracker Green CMFDA (5-chloromethylfluoroscein diacetate; Molecular Probes) according to the manufacturer's protocol at 5 hpi prior to the addition of CM-DiI-labeled target cells. In some instances, uninfected CM-DiI-labeled target cells were added at 16 hpi. At 9, 12, or 20 hpi, cells were fixed in 3% paraformaldehyde, and fluorescence was monitored and photographed with a Nikon Axiophot microscope equipped with epifluorescence and a 35-mm camera. CM-DiI emits an orange-red fluorescence, whereas the CellTracker Green CMFDA emits a green fluorescence, which allow for distinction between infected and uninfected cells as well as for cells which have fused and exhibit dual labeling.

Electron microscopy. For negative staining, virions released into culture media of infected BHK-21 or HECA2 cells were allowed to adhere to carbon-Formvar grids and stained for 15 s with 1% ammonium phosphotungstate) (pH 7.4). Specimens were viewed with a Philips CM10 transmission electron microscope.

RESULTS

Characterization of the infection of HEC and HECA2 cells by VSV. Previous observations have demonstrated that the HEC-1A cell line maintains a high state of transepithelial electrical resistance and releases enveloped viruses at distinct plasma membrane domains (3). Specifically, it was shown that

similar to other cell lines with demonstrated polarity, such as MDCK cells, influenza virus is released strictly from the apical membrane domain, while VSV is released from basolateral membrane domains. Interestingly, infection of HEC-1A cells with VSV resulted in abnormal cytopathogenicity (Fig. 1b). The most dramatic change was the appearance of multinucleated giant cells beginning at 8 to 9 hpi. The amount of fusion or giant cell formation was quantitated by determining the number of fusion events in random 20× fields compared to uninfected control cells. In addition, we calculated the number of nuclei per fusion event. Typically, a fusion event was characterized by four or more nuclei. In the parental HEC-1A cell line, the levels of fusion were approximately 10 to 30% and the number of nuclei per fusion event was approximately 10 to 15 (Fig. 1a and b). In addition, virus titers in HEC-1A cells were surprisingly very high, with yields reaching 600 PFU per cell (Fig. 2).

Since the HEC-1A cell line is a heterogeneous population of cells derived from a human endometrial adenocarcinoma, we decided to subclone this cell line to develop a more homogeneous population of cells. Subclones of the HEC-1A cell line were obtained by standard limited dilution and cloning chamber methodologies. The cell lines were further characterized based on their ability to establish high transepithelial resistance and sensitivities to virus infections. To our surprise, one of the cell lines, which we have designated HECA2, exhibited an even greater degree of giant cell formation following VSV infection. The HECA2 cell line retains many of the properties of the parental cell line, such as high transepithelial resistance and permissiveness to infection with both influenza virus and VSV. Multinucleated giant cells began to form in infected monolayers of HECA2 cells beginning at 8 hpi, and by 24 hpi large multinucleated giant cells containing approximately 50 nuclei were evident (Fig. 1c and d; Table 1). At this time, more than 80% of the nuclei were associated with giant cells (Table 1). To further investigate the nature of the VSV-induced giant cell formation, we took advantage of the high levels of giant cell formation obtained in the HECA2 cell line for all subsequent studies. As can be seen in Fig. 2, VSV replication in HECA2 cells displayed similar kinetics and produced similar yields as in the HEC-1A parental cell line.

Since VSV fusion classically requires that the viral G protein undergo a low-pH-mediated conformational change (26), we considered that the extracellular medium might become acidified as infection progressed. Alternatively, since VSV preferentially buds from the basolateral domain, a drop in the pH at this microdomain may be sufficient to render the viral G protein fusion competent. However, the pH of the extracellular media remained at pH 7 or above during all time points measured. Fusion was also observed if the cells were grown on permeable membrane supports, and we were unable to detect an acidification of the apical or basolateral bathing medium (data not shown). These results suggest that the viral G protein acquires a fusion-competent form during its transport to the cell surface.

The viral G protein is sufficient for fusion in HEC cells. To examine whether the viral G protein alone was sufficient to induce giant cell formation, we infected HECA2 cells with a vaccinia virus recombinant expressing the G protein of VSV. As expected, expression of the VSV G protein via a vaccinia virus expression vector was sufficient to induce massive cell-to-cell fusion in HECA2 cells (Fig. 1e). A recombinant vaccinia virus expressing the influenza A virus nucleoprotein failed to induce giant cell formation in these cells and was used as a negative control (data not shown). We also examined the giant cell-inducing ability of several strains of VSV as well as the giant cell formation of VSV in other polarized and nonpolarized epithelial cell types. All isolates of VSV tested, including two different isolates each of the Indiana and New Jersey serotypes, were able to induce giant cell formation in HECA2 cells, albeit to different degrees. VSV infection of the epithelial cell lines MDCK, HeLa, and A549 or the fibroblast cell line BHK-21 did not result in detectable levels of giant cell formation by VSV_{IND}. However, extensive cell rounding and cell death were observed in these cells. Together these results suggest that the giant cell-inducing phenotype is a property of the HEC epithelial cell type and is observed with various VSV isolates.

VSV giant cell formation is inhibited by neutralization of vesicular pH. It has been shown that the *trans* Golgi network is an acidic compartment in certain cell types (2). In the case of virus glycoprotein sorting, passage through acidic vesicular compartments can lead to reversible and/or irreversible conformational changes in the native proteins. In the absence of other viral proteins, some hemagglutinin (HA) subtypes of influenza A viruses undergo irreversible conformational changes during exocytosis, rendering them biologically inactive. Coexpression of these HAs with the viral M2 protein, which acts to neutralize intravesicular pH, alleviates the irreversible conformational changes to the HA and allows for expression of biologically active HA on the cell surface (54). Alterations to protein conformations which are induced by low-pH exposure can be alleviated by treatment with lysosomotropic weak bases and ionophores such as chloroquine, ammonium chloride, and monensin (33). These agents act indirectly by raising the intravesicular pH. Since cell-to-cell fusion of VSV-infected monolayers has also been demonstrated after brief exposure of the monolayers to low-pH media (17, 29, 56), we examined whether the VSV G protein undergoes a low-pH conformational change during intracellular transport in the HECA2 cell line. Thus, we monitored the level and extent of giant cell formation in the presence of increasing concentrations of NH_4Cl. To rule out any inhibitory effects of NH_4Cl on viral entry, we added the compound at 3.5 hpi.

NH_4Cl was found to inhibit giant cell formation in a concentration-dependent manner and resulted in a delay in the appearance of giant cell formation. At 1 mM NH_4Cl, both the levels (relative numbers of giant cells) and degree of fusion (no. of nuclei per giant cells) were drastically reduced (Fig. 3; Table 1). Giant cell formation was not evident at 9 hpi, but at 24 hpi small heterokaryons with approximately 15 to 20 nuclei were evident. This was similar to the result for untreated infected cells at 9 hpi, where giant cell formation was readily observed (Table 1). At 20 mM NH_4Cl, virus-induced giant cell formation was almost completely abrogated. This result adds further credence to the hypothesis that the viral G protein undergoes a low-pH-induced conformational change rendering it fusion competent during transport to the cell surface. We observed, however, that the neutral form of the G protein that is transported to the cell surface in the presence of 20 mM NH_4Cl can also be rendered fusion competent by subsequent brief treatment of these cells with pH 5.5 buffer (data not shown).

Since ammonium chloride may have affected viral glycoprotein transport and virus maturation, we also collected supernatants from infected monolayers treated with either 1 or 20 mM NH_4Cl and determined viral yields by plaque assay on BHK-21 cells. At 24 hpi, viral yields were virtually unaffected by treatment with NH_4Cl (Fig. 4). Treatment with the weak base amantidine also had little effect on virus yields but failed to inhibit virus-induced giant cell formation (data not shown). When we examined the kinetics of virus release, we observed

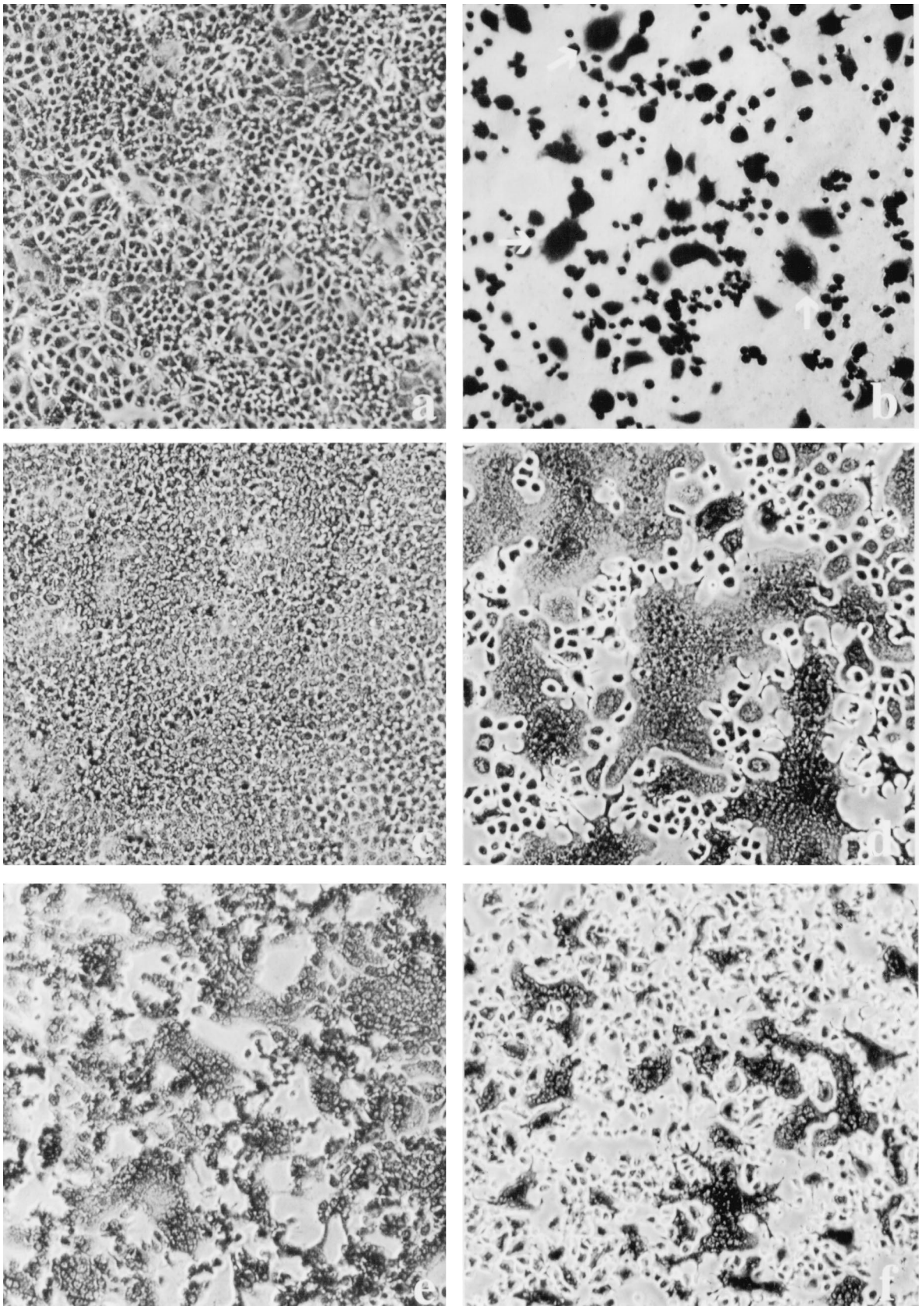

FIG. 1. VSV infection leads to polykaryon formation in HEC cell lines. Cells were infected at an MOI of 2. At 24 hpi, the monolayers were fixed in methanol and stained with Giemsa stain. (a) Mock-infected HEC-1A cells; (b) HEC-1A cells infected with VSV_{IND}; (c and d) mock- and VSV_{IND}-infected HECA2 cells, respectively; (e) HECA2 cells infected with a recombinant vaccinia virus vector encoding the full-length G protein of VSV_{IND}; (f) HECA2 cells infected with $VSV_{NJ/CA}$.

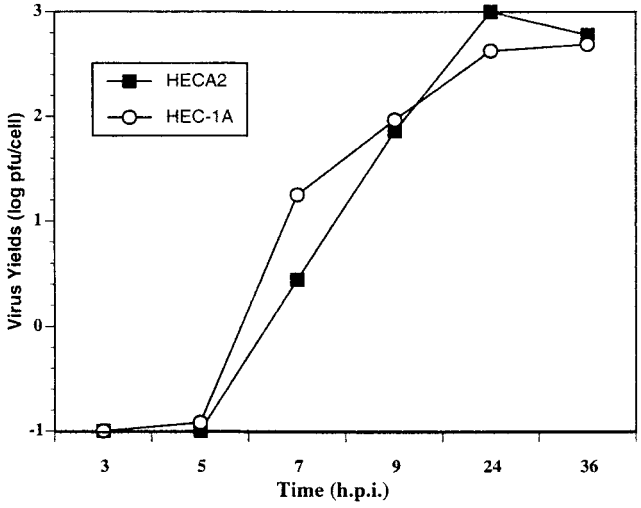

FIG. 2. Growth kinetics of VSV in HEC-1A and HECA2 cell lines. HEC cells were infected with VSV_{IND} at an MOI of 2. At different times postinfection, released virus was titrated by plaque assay. Viral yields are expressed as PFU per infected cell.

that virus yields in NH_4Cl-treated samples were approximately 50% of that of the untreated samples at 9 hpi but that with time, virus yields reached those of control cells. However, even at 36 to 48 hpi, virus-induced cell fusion was not detected in NH_4Cl-treated cells (data not shown). SDS-PAGE analysis of ^{35}S-labeled virions released into the medium in the presence of NH_4Cl failed to reveal any significant differences in protein levels or mobilities of G proteins (see Fig. 7). From these results, we can conclude that NH_4Cl treatment does not significantly affect virus maturation and release but does efficiently inhibit VSV-induced cell fusion of HEC cells.

TABLE 1. Quantitation of VSV giant cell formation in HECA2 cells

Treatment[a]	No. of S/field[b]	No. of nuclei/ synctium[c]	% Nuclei associated with S
None			
9 hpi	28	8	12.0
24 hpi	34.5	48	88.0
NH_4Cl			
1 mM	40.5	17	37.5
20 mM	0		0
Bfm A1			
1 nM	0		0
100 nM	0		0
Virus[d]			
VSV_{IND}	36	57	94
$VSV_{NJ/CA}$	60	30	83

[a] At 9 hpi, fusion was detected only in untreated cells. All other values were determined at 24 hpi.

[b] The average number of giant cells or syncytia (S) was determined by counting giant cells in random fields of 20× micrographs of DAPI-stained monolayers. Only cells with more than four nuclei per cell were considered syncytia.

[c] Determined by using the formula $(mock_n - IN_n)/N_S$, where $mock_n$ is the mean number of single nuclei determined from random fields in noninfected monolayers ($mock_n$ = 1,875), IN_n is the mean number of single nuclei per random 20× field in infected monolayers (data not shown), and N_S is the mean number of syncytia per random field.

[d] In a separate experiment, HECA2 cells were mock infected or infected with VSV_{IND} or $VSV_{NJ/CA}$. Giant cell formation was determined as described above.

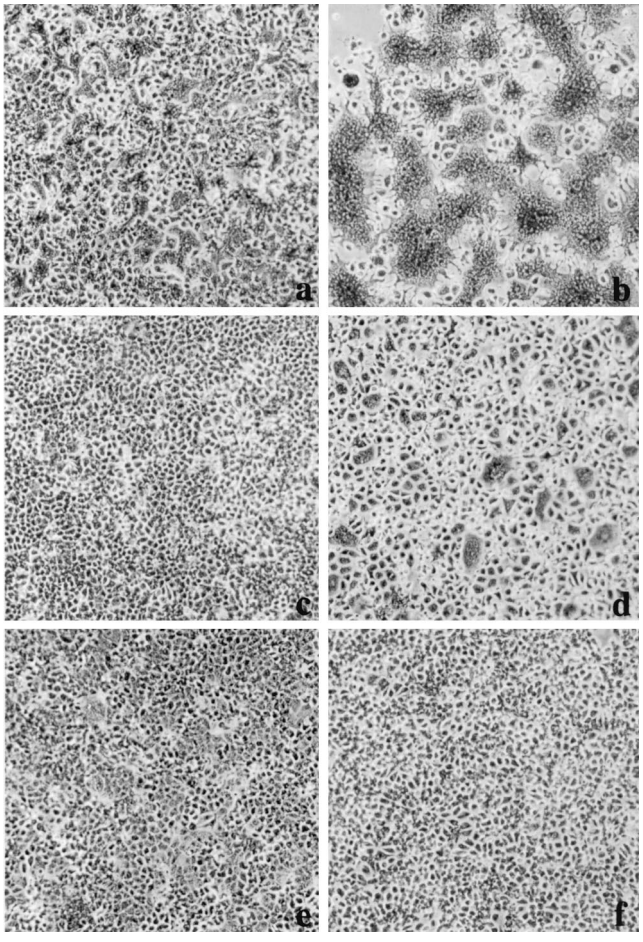

FIG. 3. Treatment with NH_4Cl ablates fusion from within. VSV_{IND}-infected HECA2 cells (MOI = 2) were cultured in the presence of 1 and 20 mM NH_4Cl beginning at 3.5 hpi. At 9 (a, c, and e) and 24 (b, d, and f) hpi, the cells were fixed in methanol and stained with Giemsa stain. Giant cell formation was observed and recorded with an Nikon TMD microscope equipped with a 35-mm camera. (a and b) Untreated VSV_{IND}-infected HECA2 cells; (c and d) infected HECA2 cells treated with 1 mM NH_4Cl; (e and f) infected HECA2 cells treated with 20 mM NH_4Cl.

Inhibition of cell-to-cell fusion by the vacuolar H^+-ATPase inhibitor Bfm A1. Intravesicular pH can be regulated by several enzymes and proton pumps. Among these, the vacuolar H^+-ATPase is perhaps the most significant with respect to pH-mediated viral entry mechanisms, since it is a component of endosomal and lysosomal membranes. To examine whether an active vacuolar H^+-ATPase was also responsible for lowering the pH of exocytotic transport vesicles, we analyzed the effects of Bfm A1 on the replication, transport, and release mechanisms of VSV. Bfm A1 is a very potent and specific inhibitor of H^+-vacuolar ATPases which does not affect other ATPases, such as mitochondrial F-class ATPases or plasma membrane H^+-ATPases of the P class (35, 49).

In VSV-infected HECA2 cells treated with Bfm A1, we observed an almost complete inhibition of giant cell formation at a Bfm A1 dose as low as 1 nM (Fig. 5a). As observed in NH_4Cl-treated cells, the VSV G protein is fully fusogenic in Bfm A1-treated cells following low-pH exposure (Fig. 5d), as evidenced by the pronounced loss of demarcation between

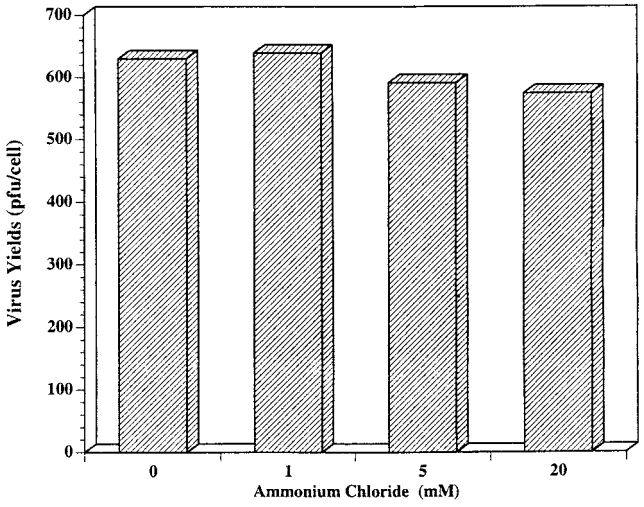

FIG. 4. Ammonium chloride does not affect viral yields. HECA2 cells were infected with VSV_{IND} at an MOI of 2 and cultured in the presence or absence of ammonium chloride essentially as described in the legend to Fig. 3. At 24 hpi, the virus released from HECA2 cells was titrated by plaque assay in BHK-21 cells and expressed as PFU per cell.

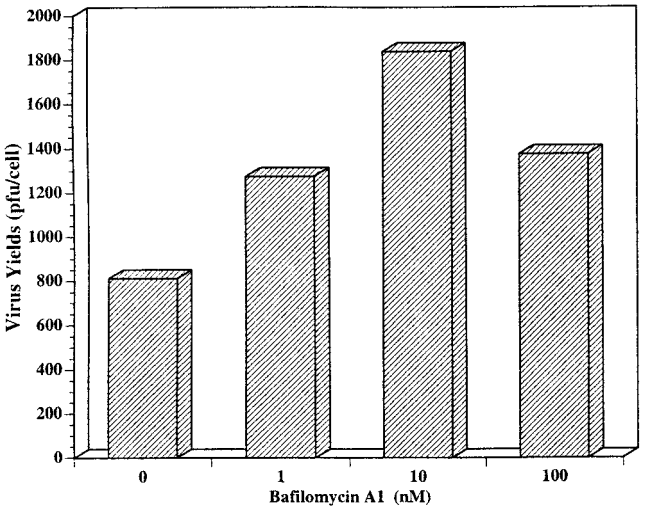

FIG. 6. Bfm A1 does not inhibit virus yield. Following a 24-h infection with VSV_{IND} either in the presence or in the absence of different concentrations of Bfm A1, the virus released from HECA2 cells was titrated by plaque assay in BHK-21 cells. Virus yields are expressed as PFU per cell.

fused cells (see also Fig. 8). Thus, a block in transport due to drug treatment is not responsible for inhibition of fusion. In agreement with this observation, the kinetics of virus replication and viral yields in the presence of Bfm A1 were very similar to those for untreated infected cells, which further argues against a drug-induced defect in viral transport or assembly (Fig. 6 and data not shown). Surprisingly, we found that virus yields were actually enhanced in the presence of Bfm A1.

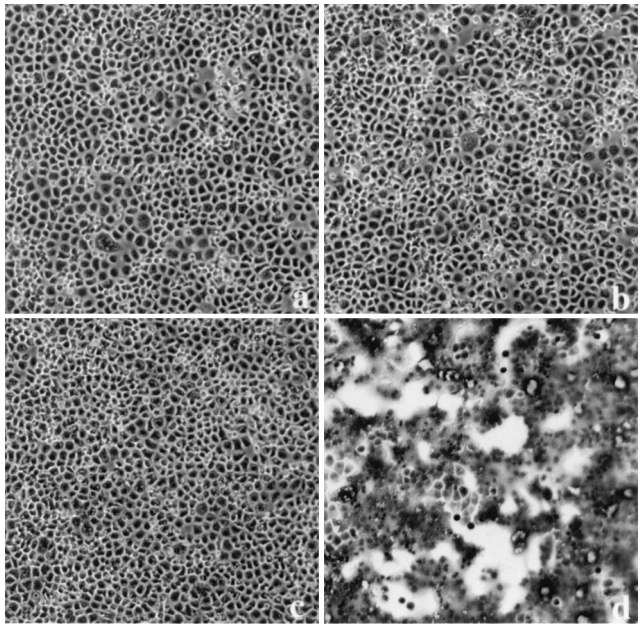

FIG. 5. Treatment with the vacuolar H^+-ATPase inhibitor Bfm A1 inhibits VSV-induced giant cell formation. VSV_{IND}-infected HECA2 cells (MOI = 2) were treated with different concentrations of Bfm A1 beginning at 3.5 hpi. At 24 hpi, the cells were fixed in methanol and stained with Giemsa stain. Giant cell formation was completely inhibited at 1, 10, and 100 nM Bfm A1 (a, b, and c, respectively). Giant cell formation could be induced in 10 nM Bfm A1-treated cells following a brief exposure to pH 5.5 buffer (d).

A more neutral form of the viral G protein may be necessary for efficient virus assembly to occur. As was observed in NH_4Cl-treated cells, Bfm A1 treatment did not appear to affect incorporation of G protein into released virions (Fig. 7). Although less viral protein appeared to be released in drug-treated cells, the ratio of the viral M to G proteins remained similar. Thus, drug treatment did not significantly affect viral G incorporation into virions. One possibility is that in the presence of Bfm A1, the specific infectivity of released virions is higher, which might explain why higher yields but less viral protein were observed. In agreement with these observations, electron microscopy of negatively stained virions released from Bfm A1-treated cells confirmed that the viral G glycoprotein was in fact incorporated into virions, as evidenced by the spike-like protrusions surrounding the bullet-shaped virions (data not shown). We detected no obvious differences in virus morphology due to drug treatment.

It is possible that drug treatment leads to lower levels or an altered distribution of the viral G protein at the cell surface, which would restrict giant cell formation. To address this possibility, we compared the cell surface distribution of the viral G protein both in the presence and absence of drug treatment in HECA2 cells as well as in the polarized epithelial cell lines MDCK and Vero C1008 and the fibroblast cell line BHK-21 (Fig. 8 and data not shown). We observed no significant differences in the cell surface distribution of the viral G protein

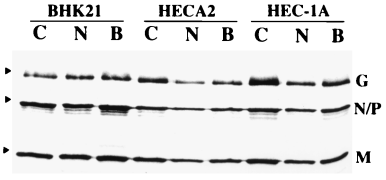

FIG. 7. Incorporation of viral proteins into virions in the presence or absence of Bfm A1 and NH_4Cl. BHK-21, HECA2, or HEC-1A cells were infected with VSV_{IND} at an MOI of 5. Beginning at 3 hpi, the cells were cultured in either 10 nM Bfm A1 or 20 mM NH_4Cl. Infected cells were metabolically labeled with 60 μCi of [^{35}S]Met-Cys per ml from 5 to 20 hpi. ^{35}S-labeled virus released into the medium was pelleted by ultracentrifugation and analyzed by SDS-PAGE. Lanes: C, control untreated cells; N, NH_4Cl-treated cells; B, Bfm A1-treated cells.

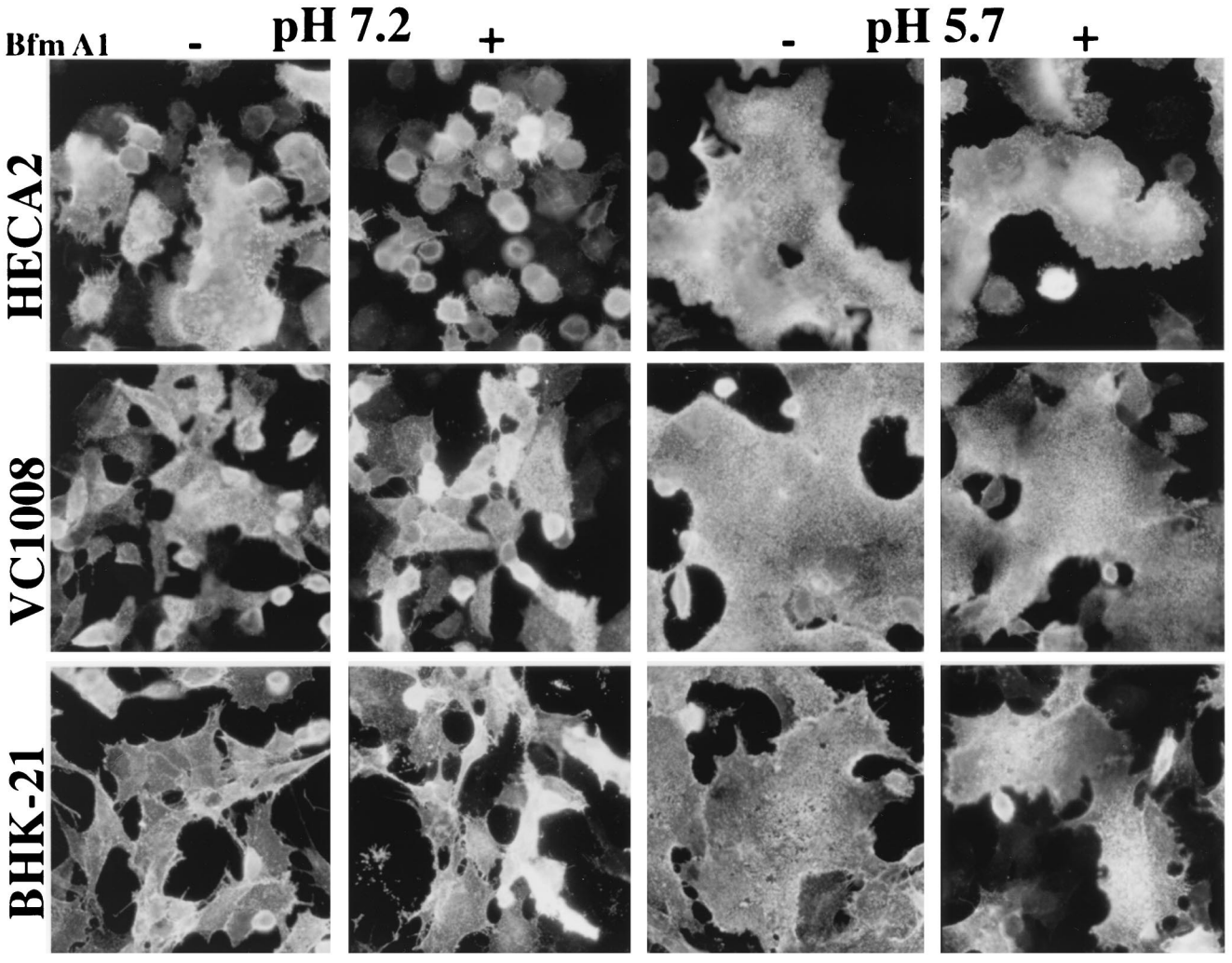

FIG. 8. Cell surface distribution and fusion activity of the viral G protein following Bfm A1 treatment. HECA2, BHK-21, and Vero C1008 cells at subconfluent cell density were infected with VSV_{IND} at an MOI of 2. Beginning at 3 hpi, the cells were cultured either in the presence (+) or in the absence (−) of 5 nM Bfm A1. At 9 hpi, the cells were briefly exposed to either low pH (pH 5.7) or neutral pH (pH 7.2) as indicated for 1 min at room temperature, subsequently neutralized with incubation medium, and incubated for a further 15 to 20 min at 37°C. Cells were fixed in 3% paraformaldehyde, and viral G protein was detected at the cell surface by using a mouse monoclonal antibody to the viral G protein followed by incubation with an Alexa 488-conjugated goat anti-mouse immunoglobulin secondary antibody. Fluorescence was monitored and photographed with a Nikon Axiophot microscope equipped with epifluorescence and a 35-mm camera.

either in the presence or in the absence of Bfm A1 (Fig. 8). To further confirm that the viral G protein expressed at the cell surface in the absence or presence of Bfm A1 was expressed at levels sufficient to initiate cell fusion, drug-treated cells were briefly exposed to low-pH (pH 5.7) buffer and subsequently neutralized with incubation medium. Infected cells treated with Bfm A1 underwent rapid cell fusion (within 15 to 20 min) with neighboring cells (Fig. 8). This result confirms that in Bfm A1-treated cells, the viral G protein is expressed at the cell surface in quantities sufficient to induce giant cell formation if triggered by exogenous low-pH treatment.

To confirm that the low pH encountered during transport was not an artifact due to a transient drop in the pH of the incubation medium, we analyzed cell fusion between subconfluent HECA2 cells infected with VSV_{IND} and different uninfected target cell lines (Fig. 9). To ablate intracellular exposure of the viral G protein to low pH, cells were again incubated in the presence of Bfm A1. The pH of the incubation media was monitored throughout the infection to rule out a transitory drop in pH. To distinguish between infected and uninfected cells following giant cell formation, we fluorescently labeled both infected and target cells with the fluorescent tracking dyes CellTracker Green and CM-DiI, respectively. Thus, uninfected cells exhibit a red-orange fluorescence and infected cells exhibit a green fluorescence, making them highly distinguishable.

When uninfected HECA2 cells were used as target cells, cell-cell fusion was readily observed at 8 to 9 hpi, as revealed by the presence of both fluorochromes within individual giant cells (Fig. 9). It should be noted that no detectable leakage of dye occurred between cell lines. Surprisingly, when infected monolayers were incubated overnight prior to the addition of target cells, they were still able to fuse with uninfected target cells, even though they had already formed giant cells with neighboring cells (data not shown). This finding suggests that giant cells still express viral G protein in a fusion-competent conformation at the cell surface. Interestingly, we found that uninfected HECA2 cells appeared to be more susceptible to cell-cell fusion with infected cells (Fig. 9a to c) than BHK-21 or

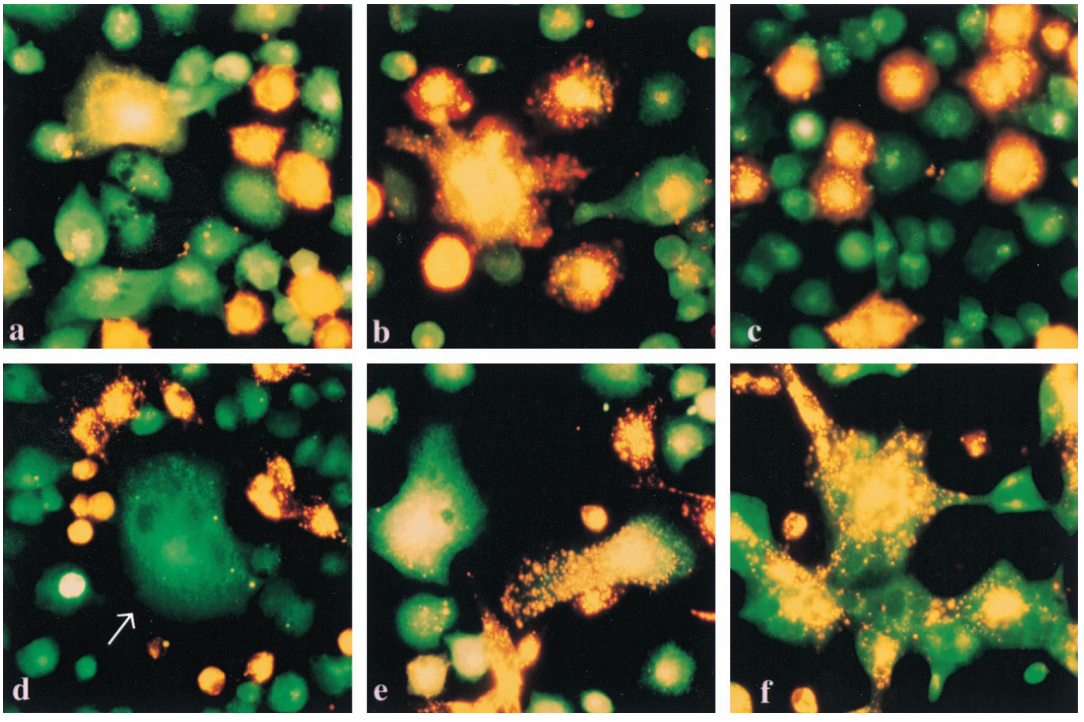

FIG. 9. VSV-infected HECA2 cells can induce fusion with uninfected target cells. Subconfluent monolayers of HECA2 cells were infected with VSV_{IND} at an MOI of 2. Beginning at 3 hpi, the cells were cultured either in the presence or in the absence of 5 nM Bfm A1. Infected HECA2 cell monolayers were labeled with CellTracker Green CMFDA (green fluorescence) for 40 min at 37°C at 5 hpi. Uninfected target cells, HECA2 (a to c) or BHK-21 (d to f), were labeled with the lipophilic fluorochrome CM-DiI (red-orange fluorescence), trypsinized, and added to the infected cell monolayers at 6.5 hpi. Giant cell formation was monitored from 6 to 12 hpi, at which time monolayers were fixed in 3% paraformaldehyde. Fluorochrome distribution was monitored and photographed with a Nikon Axiophot microscope equipped with epifluorescence and a 35-mm camera. (a and b) HECA2-HECA2 cell fusion at 9 and 12 hpi, respectively (pH 7.2 in the absence of Bfm A1); (c) inhibition of HECA2-HECA2 cell fusion by treatment with Bfm A1 (12 hpi); (d) HECA2-BHK21 cell fusion at 9 hpi (pH 7.2, no Bfm A1); (e and f) HECA2-BHK21 cell fusion at 12 hpi at pH 7.2 and 5.7, respectively. The arrow in panel d points to giant cell formation between infected HECA2 cells.

MDCK cells. However, BHK-21 cells could serve as potential targets for cell-cell fusion at later time points, albeit at significantly lower levels (Fig. 9d to f). Presumably the HECA2 cells are more compatible in establishing cell-cell contact regions with each other than with other cell types. As expected, HECA2 cells treated with Bfm A1 were unable to initiate fusion with target cells (Fig. 9c) unless they were exposed exogenously to low pH (data not shown), again confirming that drug treatment was maintaining the viral G protein in a neutral nonfusogenic conformation during exocytotic transport (see also Fig. 8). Thus, we conclude that bafilomycin A1 prevents the conformational change which activates fusion activity, without affecting transport of the G protein to the cell surface.

Together, the results presented here support the hypothesis that in HEC cells the VSV G protein can acquire a fusion-competent form during exocytotic transport and that this conformation is mediated by intracellular exposure to low pH.

DISCUSSION

The results presented here show that VSV can induce cell fusion in an epithelial cell line without exogenous exposure to a low-pH environment. Our data suggest that cell fusion activity is actually a result of a low-pH-mediated conformational change in the viral G protein, acquired as it traverses the exocytotic transport pathway. Our results show that VSV G protein-induced giant cell formation is readily inhibited by treatment with the weak lysosomotropic base NH_4Cl. In addition, the results with Bfm A1 suggest that an active vacuolar H^+-ATPase is required for maintaining the low intravesicular pH during transport to the cell surface. We did not observe any significant defects in transport of viral proteins or release of VSV virions into the medium in the presence of these compounds, suggesting that drug treatment was specifically acting to neutralize intravesicular pH levels during transport of the viral G protein to the cell surface.

During the course of VSV infection, HEC cells gradually fuse to form large multinucleated giant cells. This apparent fusion from within, or fusion of virus infected cells with neighboring cells, is not a usual event in the life cycle of VSV. Generally, VSV is considered to be highly cytocidal, resulting in rapid cell rounding and eventual cell death. This is thought to occur in part via virus-mediated disassembly of the host cell cytoskeleton (30, 47, 52). The HECA2 subclone appears to be more resistant to the cytopathic effects of VSV infection. Cell rounding, which occurs rapidly (ca. 4 to 6 hpi) in BHK-21 cells (30, 52), does not occur as rapidly in the HECA2 cells. This may allow the G protein to accumulate at microdomains at the plasma membrane that then initiate cell-to-cell membrane fusion. This may be one reason why these cells fuse more efficiently than the parental HEC-1A cell line, which appears to be more sensitive to cell rounding upon infection. In agreement with previous observations (52), we also observed microfilament disassembly in HEC cell lines following infection, but it occurred much more slowly than in BHK-21 cells (data not shown). Although the resistance to cytopathicity may contribute to enhanced fusion activity in HEC cells, it is clearly evident that the viral G protein must first undergo a low-pH-mediated conformational change in order to initiate fusion.

The prerequisites for virus-induced giant cell formation are

still poorly understood. While it is clear that cellular receptors are necessary, the lipid constituents of the host cell plasma membrane may also play an important role (44–46). Manipulation of the extent of acyl-chain saturation can be used to control virus-induced cell fusion in a number of different cell lines (46). In addition, lipid-supplemented media can be used to control fusogenic responses of cells to chemical fusogens (45). It seems highly unlikely that NH_4Cl or Bfm A1 treatment would exert such an effect on lipid composition, rendering cells resistant to virus-mediated fusion. The differences observed between HEC and the cloned HECA2 cell line may be the result of different concentrations of vacuolar H^+-ATPases in the vesicular exocytotic transport machinery. Previous reports have shown that vacuolar H^+-ATPases are involved in the entry process of several different viruses that require low-pH-dependent entry mechanisms for infection to occur (38, 39). The highly specific vacuolar H^+-ATPase inhibitor Bfm A1 was found to inhibit entry of such viruses as influenza virus, VSV, and Semliki Forest virus, all of which require a low-pH-mediated entry step (39). In contrast, virus entry by Sendai virus, a member of the *Paramyxoviridae* family which can initiate fusion at neutral pH, or by vaccinia virus was not effected by Bfm A1 treatment (39). We found that Bfm A1 was equally effective in preventing entry of VSV derived from either BHK-21 or HECA2 cells (data not shown). This finding also indicates that the VSV that is released from HECA2 cells requires low pH to activate its fusion activity, suggesting that the viral G protein has reverted to a neutral nonfusogenic form during or after release. However, we did find that higher concentrations of Bfm A1 were needed to completely inhibit entry of VSV in HEC and BHK-21 cells: 100 to 500 nM, compared to 1 to 10 nM Bfm A1 needed to prevent giant cell formation. This may indicate that the vacuolar H^+-ATPase is more concentrated in endocytotic vesicles, thus requiring greater concentrations of Bfm A1 to abrogate function. Alternatively, different isomers of vacuolar H^+-ATPase may exist in different intracellular compartments (24).

A role of vacuolar H^+-ATPases in exocytotic transport of viral proteins has been described for Semliki Forest virus and VSV infection of BHK-21 cells (38); the authors reported that viral glycoprotein transport and virus maturation can be blocked by treatment with Bfm A1. In contrast, our results indicate that Bfm A1 does not significantly affect VSV maturation or release in HECA2 cells. We observed no significant differences between control and drug-treated cells with respect to the distribution of the virus G protein at the cell surface. In addition, the kinetics of VSV release were not found to be altered in response to low concentrations of Bfm A1, even though cell-to-cell fusion was completely abrogated. It should be noted that in the previous studies (38, 39), Bfm A1 was used at concentrations higher (100 to 500 nM) than we employed. These higher concentrations may have a more generalized effect on cellular transport machinery in BHK-21 cells, which may remain functional in the HEC cells at the lower concentrations used here. In fact, in BHK-21 cells treated with Bfm A1, dilation and vacuolization of the Golgi apparatus was observed (38). Another explanation for the observed differences may lie in the fact that HECA2 is a polarized epithelial cell line whereas BHK-21 cells are of fibroblast origin. Vacuolar H^+-ATPase compartmentalization may differ between epithelial and fibroblast cell lineages.

It is not unusual for viral glycoproteins to encounter low-pH environments during exocytotic transport. Influenza A virus HAs of some strains which are cleaved intracellularly acquire a low-pH-defective conformation when expressed without the viral M2 protein or in the presence of amantidine (6, 25, 54, 55). The coexpression of the viral M2 protein neutralizes vesicular pH during exocytotic transport, maintaining the viral HA in an inactive, neutral conformation (55). Both ammonium chloride and chloroquine can alleviate the effects of low-pH exposure on HA conformation observed in the absence of the M2 protein (37). Thus, influenza A viruses have evolved with helper proteins, which help to regulate intravesicular pH during transport of viral glycoproteins. In the case of VSV G protein, unlike influenza virus HA, the low-pH-induced conformational change leading to activation of fusion activity appears to be readily reversible, as demonstrated in our studies as well as previous reports (4, 5, 41). Therefore, the glycoproteins of these viruses are able to undergo transport through intravesicular acidic compartments without an irreversible conformational change which could lead to inactivation of their biological function. Similarly, HAs from other strains of influenza virus reach the cell surface without prior cleavage-activation of the HA. Expression in the absence of the viral M2 protein does not appear to lead to irreversible conformational changes in these HAs during transport. These uncleaved HAs are individually expressed as biologically active molecules once they are proteolytically activated at the cell surface (37, 41). Thus, the uncleaved precursor appears to be more resistant to the acid environment of the exocytotic pathway than the cleaved protein. Likewise, acid-stabile mutants of influenza virus HA are able to retain functional activity when M2 function is ablated by amantidine treatment (53).

The rabies virus G glycoprotein has also been reported to undergo low-pH-induced conformational changes during transport (21, 23, 57). It has been proposed that the rabies virus G protein undergoes a series of transitional intermediates during transport (20, 21). In the Golgi apparatus, the G protein undergoes a conformational transition that is triggered by low pH to the inactive form. This transitional state presumably protects the G protein from unwanted intracellular fusion with acidic vesicles. The viral G protein is then thought to shift back to a more native state close to or at the cell surface. The VSV G protein may undergo a similar transition during transport in HECA2 cells. The VSV-G fusion-competent form is likely just an intermediate, since released virions do not appear to possess intrinsic fusion activity. Thus, we favor a mechanistic view of cell fusion in HECA2 cells whereby the VSV G protein undergoes transitory conformational changes as it traverses the exocytotic transport machinery. First, the G protein acquires a low-pH form during exocytotic transport, probably in Golgi compartments. This low-pH form is expressed on the cell surface and can induce syncytium formation but gradually transitions back to the native or neutral state after it is expressed at the cell surface or incorporated into virions. The rhabdovirus G proteins are homotrimeric transmembrane proteins (22, 27). There also appears to be constant interchange between G monomers and oligomers at equilibrium (58). Interestingly, the oligomeric state of the VSV G protein can be stabilized at low pH (12, 15), which also renders it resistant to proteolytic digestion by trypsin (19). The VSV G protein isolated from HECA2-infected cells was fully sensitive to trypsin digestion when lysed in pH 7.0 buffer, whereas it was completely protected against degradation when lysed in pH 5.5 buffer. This finding suggests that the low-pH, fusion-competent form of the VSV G protein in HECA2 cells can readily revert to the neutral, trypsin-sensitive form.

Acquiring a fusion-competent form at or near the cell surface may allow the virus to spread from cell to cell without the need for virion release. This might allow the virus to escape the effects of neutralizing antibody. Interestingly, antibody escape mutants of rabies virus with altered virulence have been iso-

lated (10, 11). These virulent escape mutants support cell-to-cell spread of infection in the presence of neutralizing antiserum, whereas the nonvirulent mutants were significantly delayed in replication kinetics (13). In vivo, infection of the mouse brain spreads more rapidly with pathogenic or virulent mutants than during infection by nonpathogenic mutants (13). Interestingly, Morimoto and coworkers (34) have presented evidence that the virulent escape mutants are able to initiate pH-independent syncytium formation in certain neuroblastoma cell lines (34). This may suggest that acquisition of a fusion-competent form of the viral G protein in vivo will aid in progression of infection in certain tissues. Therefore, the HECA2 cell line is of interest for further investigation of the role of host cell components in promoting virus-induced cell-to-cell fusion.

ACKNOWLEDGMENTS

We express our gratitude to Lawrence Melsen for help with photography and electron microscopy. We also thank Stuart Nichol (CDC, Atlanta, Ga.) for kindly providing recent isolates of VSV.

This study was supported by NIH grant CA18611.

REFERENCES

1. **Alonso-Caplen, F. V., and R. W. Compans.** 1983. Modulation of glycosylation and transport of viral membrane glycoproteins by a sodium ionophore. J. Cell Biol. **97:**659–668.
2. **Anderson, R. G., and R. K. Pathak.** 1985. Vesicles and cisternae in the trans Golgi apparatus of human fibroblasts are acidic compartments. Cell **40:**635–643.
3. **Ball, J. M., Z. Moldeveanu, L. R. Melsen, P. Kowalski, S. Jackson, M. Mulligan, J. Mestecky, and R. W. Compans.** 1995. A polarized human endometrial cell line which binds and transports polymeric IgA. In Vitro **31:**197–207.
4. **Blumenthal, R., A. Bali-Puri, A. Walter, D. Covell, and O. Eidelman.** 1987. pH-dependent fusion of vesicular stomatitis virus with vero cells. J. Biol. Chem. **262:**13614–13619.
5. **Brown, J. C., W. W. Newcomb, and S. Lawrenz-Smith.** 1988. pH-dependent accumulation of the vesicular stomatitis virus glycoprotein at the ends of intact virions. Virology **167:**625–629.
6. **Ciampor, F., P. M. Baley, M. V. Nermut, E. M. A. Hirst, R. J. Sugrue, and A. J. Hay.** 1992. Evidence that the amantidine-induced, M2-mediated conversion of influenza A virus hemagglutinin to the low pH conformation occurs in an acidic trans Golgi compartment. Virology **186:**14–24.
7. **Clague, M. J., C. Schoch, L. Zech, and R. Blumenthal.** 1990. Gating kinetics of pH-activated membrane fusion of vesicular stomatitis virus with cells: stopped-flow measurements by dequenching of octadecylrhodamine fluorescence. Biochemistry **29:**1303–1308.
8. **Cleverley, D. Z., and J. Lenard.** 1998. The transmembrane domain in viral fusion: essential role for a conserved glycine residue vesicular stomatitis virus G protein. Proc. Natl. Acad. Sci. USA **95:**3425–3430.
9. **Coll, J. M.** 1995. The glycoprotein G of rhabdoviruses. Arch. Virol. **140:**827–851.
10. **Coulon, P., P. Rollin, M. Aubert, and A. Flamand.** 1982. Molecular basis of rabies virus virulence. I. Selection of avirulent mutants of the CVS strain with anti-G monoclonal antibodies. J. Gen. Virol. **61:**97–100.
11. **Coulon, P., P. E. Rollin, and A. Flamand.** 1983. Molecular basis of rabies virus virulence. II. Identification of a site on the CVS glycoprotein associated with virulence. J. Gen. Virol. **64:**693–696.
12. **Crise, B., A. Ruusal, P. Zagouras, A. Shaw, and J. K. Rose.** 1989. Oligomerization of glycolipid-anchored and soluble forms of the vesicular stomatitis virus glycoprotein. J. Virol. **63:**5328–5333.
13. **Dietzschold, B., T. J. Wiktor, J. Q. Trojanowski, R. I. Macfarlan, W. H. Wunner, M. J. Torres-Anjel, and H. Koprowski.** 1985. Differences in cell-to-cell spread of pathogenic and apathogenic rabies virus in vivo and in vitro. J. Virol. **56:**12–18.
14. **Dille, B. J., and T. C. Johnson.** 1982. Inhibition of vesicular stomatitis virus glycoprotein expression by chloroquine. J. Gen. Virol. **62:**91–103.
15. **Doms, R. W., and A. Helenius.** 1988. Properties of a viral fusion protein, p. 385–398. *In* D. D. S. Ohki, T. D. Flanagan, S. W. Hui, and E. Mayhew (ed.), Molecular mechanisms of membrane fusion. Plenum, New York, N.Y.
16. **Durrer, P., Y. Gaudin, R. W. Ruigrok, R. Graf, and J. Brunner.** 1995. Photolabeling identifies a putative fusion domain in the envelope glycoprotein of rabies and vesicular stomatitis viruses. J. Biol. Chem. **270:**17575–17581.
17. **Florkiewicz, R. Z., and J. K. Rose.** 1984. A cell line expressing vesicular stomatitis virus glycoprotein fuses at low pH. Science **225:**721–723.
18. **Fredericksen, B. L., and M. A. Whitt.** 1998. Attenuation of recombinant vesicular stomatitis viruses encoding mutant glycoproteins demonstrate a critical role for maintaining a high pH threshold for membrane fusion in viral fitness. Virology **240:**349–358.
19. **Fredricksen, B. L., and M. A. Whitt.** 1996. Mutations at two conserved acidic amino acids in the glycoprotein of vesicular stomatitis virus affect pH-dependent conformational changes and reduce the pH threshold for membrane fusion. Virology **217:**49–57.
20. **Gaudin, Y., H. Raux, A. Flamand, and R. W. Ruigrok.** 1996. Identification of amino acids controlling the low-pH-induced conformational change of rabies virus glycoprotein. J. Virol. **70:**7371–7378.
21. **Gaudin, Y., R. W. Ruigrok, M. Knossow, and A. Flamand.** 1993. Low-pH conformational changes of rabies virus glycoprotein and their role in membrane fusion. J. Virol. **67:**1365–1372.
22. **Gaudin, Y., R. W. H. Ruigrok, C. Tuffereau, M. Knossow, and A. Flamand.** 1992. Rabies virus glycoprotein is a trimer. Virology **187:**627–632.
23. **Gaudin, Y., C. Tuffereau, P. Durrer, A. Flamand, and R. W. H. Ruigrok.** 1995. Biological function of the low-pH, fusion-inactive conformation of rabies virus glycoprotein (G): G is transported in a fusion-inactive state-like conformation. J. Virol. **69:**5528–5534.
24. **Gluck, S. L.** 1993. The vacuolar H+-ATPases: versatile proton pumps participating in constitutive and specialized functions of eukaryotic cells. Int. Rev. Cytol. **137:**105–137.
25. **Grambas, S., M. S. Bennett, and A. J. Hay.** 1992. Maturation of influenza A virus hemagglutinin—estimates of the pH encountered during transport and its regulation by the M2 protein. Virology **190:**11–18.
26. **Hernandez, L. D., L. R. Hoffman, T. G. Wolfsberg, and J. M. White.** 1996. Virus-cell and cell-cell fusion. Annu. Rev. Cell Dev. Biol. **12:**627–661.
27. **Kreis, T. E., and H. F. Lodish.** 1986. Oligomerization and is essential for transport of the vesicular stomatitis virus glycoprotein to the cell surface. Cell **46:**929–937.
28. **Laemmli, U. K.** 1970. Cleavage of structural proteins during the assembly of the head of bacteriophage T4. Nature (London) **277:**680–685.
29. **Li, Y., C. Drone, E. Sat, and H. P. Ghosh.** 1993. Mutational analysis of the vesicular stomatitis virus glycoprotein G for membrane fusion domains. J. Virol. **67:**4070–4077.
30. **Lyles, D. S., and M. O. Mckenzie.** 1997. Activity of vesicular stomatitis virus M protein mutants in cell rounding is correlated with the ability to inhibit host gene expression and is not correlated with virus assembly function. Virology **229:**77–89.
31. **Marsh, M., and A. Helenius.** 1989. Virus entry into animal cells. Adv. Virus Res. **36:**107–151.
32. **Matlin, K. S., H. Reggio, A. Helenius, and K. Simons.** 1982. Pathway of vesicular stomatitis virus entry leading to infection. J. Mol. Biol. **156:**609–631.
33. **Mellman, I., R. Fuchs, and A. Helenius.** 1986. Acidification of the endocytic and exocytic pathways. Annu. Rev. Biochem. **55:**663–700.
34. **Morimoto, K., Y. J. Ni, and A. Kawai.** 1992. Syncytium formation is induced in the murine neuroblastoma cell cultures which produce pathogenic type G proteins of the rabies virus. Virology **189:**203–216.
35. **Nelson, W. J., and R. W. Hammerton.** 1989. A membrane cytoskeletal complex containing Na+, K+-ATPase, ankyrin, fodrin in Madin-Darby canine kidney (MDCK) cells: implications for the biogenesis of epithelial cell polarity. J. Cell Biol. **108:**893–903.
36. **Odell, D., E. Wanas, J. Yan, and H. P. Ghosh.** 1997. Influence of membrane anchoring and cytoplasmic domains on the fusogenic activity of vesicular stomatitis virus glycoprotein G. J. Virol. **71:**7996–8000.
37. **Ohuchi, M., A. Cramer, M. Vey, R. Ohuchi, W. Garten, and H.-D. Klenk.** 1994. Rescue of vector-expressed fowl plague virus hemagglutinin in biologically active form by acidotropic agents and coexpressed M2 protein. J. Virol. **68:**920–926.
38. **Palokangas, H., K. Metsikko, and K. Vaananen.** 1994. Active vacuolar H+-ATPase is required for both endocytic and exocytic processes during viral infection of BHK-21 cells. J. Biol. Chem. **269:**17577–17585.
39. **Perez, L., and L. Carrasco.** 1994. Involvement of the vacuolar H+-ATPase in animal virus entry. J. Gen. Virol. **75:**2595–2606.
40. **Puri, A., S. Grimaldi, and R. Blumenthal.** 1992. Role of viral envelope sialic acid in membrane fusion mediated by the vesicular stomatitis virus envelope glycoprotein. Biochemistry **31:**10108–10113.
41. **Puri, A., J. Winick, R. J. Lowy, D. Covell, O. Efferman, A. Walter, and R. Blumenthal.** 1988. Activation of vesicular stomatitis virus fusion with cells by pretreatment at low pH. J. Biol. Chem. **263:**4749–4753.
42. **Riedel, H., C. Kondor-Koch, and H. Garoff.** 1984. Cell surface expression of fusogenic vesicular stomatitis virus G protein from cloned cDNA. EMBO J. **3:**1477–1483.
43. **Rigaut, K. D., D. E. Birk, and J. Lenard.** 1991. Intracellular distribution of input vesicular stomatitis virus proteins after uncoating. J. Virol. **65:**2622–2628.
44. **Roos, D. S., and P. W. Choppin.** 1985. Biochemical studies on cell fusion. I. Lipid composition of fusion-resistant cells. J. Cell Biol. **101:**1578–1590.
45. **Roos, D. S., and P. W. Choppin.** 1985. Biochemical studies on cell fusion. II. Control of fusion response by lipid alteration. J. Cell Biol. **101:**1591–1598.

46. **Roos, D. S., C. S. Duchala, C. B. Stephensen, K. V. Holmes, and P. W. Choppin.** 1990. Control of virus-induced cell fusion by host cell lipid composition. Virology **175:**345–357.
47. **Rutter, G., and K. Mannweiler.** 1977. Alterations of actin-containing structures in BHK-21 cells infected with Newcastle disease virus and vesicular stomatitis virus. J. Gen. Virol. **37:**233–242.
48. **Schlegel, R., T. S. Tralka, M. C. Willingham, and I. Pastan.** 1983. Inhibition of VSV binding and infectivity by phosphatidylserine: is phosphatidylserine a VSV binding site? Cell **32:**639–646.
49. **Schneider, R. J., and T. Shenk.** 1987. Impact of virus infection on host cell protein synthesis. Annu. Rev. Biochem. **56:**317–332.
50. **Shokralla, S., R. Chernish, and H. P. Ghosh.** 1999. Effects of double-site mutations of vesicular stomatitis virus glycoprotein G on membrane fusion activity. Virology **256:**119–129.
51. **Shokralla, S., Y. He, E. Wanas, and H. P. Ghosh.** 1998. Mutations in a carboxy-terminal region of vesicular stomatitis virus glycoprotein G that affect membrane fusion activity. Virology **242:**39–50.
52. **Simon, K. O., P. A. Whitaker-Dowling, J. S. Younger, and C. C. Widnell.** 1990. Sequential disassembly of the cytoskeleton in BHK-21 cells infected with vesicular stomatitis virus. Virology **177:**289–297.
53. **Steinhauer, D. A., S. A. Wharton, J. J. Skehel, D. C. Wiley, and A. J. Hay.** 1991. Amantidine selection of a mutant influenza virus containing an acid-stable hemagglutinin glycoprotein: evidence for virus-specific regulation of the pH of glycoprotein transport vesicles. Proc. Natl. Acad. Sci. USA **88:** 11525–11529.
54. **Sugrue, R. J., G. Bahadur, M. C. Zambon, M. Hall-Smith, A. R. Douglas, and A. J. Hay.** 1990. Specific alteration of the influenza hemagglutinin by amantadine. EMBO J. **9:**3469–3476.
55. **Takeuchi, K., and R. A. Lamb.** 1994. Influenza virus M2 protein ion channel activity stabilizes the native form of fowl plague virus hemagglutinin during intracellular transport. J. Virol. **68:**911–919.
56. **White, J., K. Matlin, and A. Helenius.** 1981. Cell fusion by Semliki forest, influenza, and vesicular stomatitis viruses. J. Cell Biol. **89:**674–679.
57. **Whitt, M. A., L. Buonocore, C. Prehaud, and J. K. Rose.** 1991. Membrane fusion activity, oligomerization, and assembly of the rabies virus glycoprotein. Virology **185:**681–688.
58. **Zagouras, P., and J. K. Rose.** 1993. Dynamic equilibrium between vesicular stomatitis virus glycoprotein monomers and trimers in the Golgi and at the cell surface. J. Virol. **67:**7533–7538.
59. **Zhang, L., and H. P. Ghosh.** 1994. Characterization of the putative fusogenic domain in vesicular stomatitis virus glycoprotein G. J. Virol. **68:**2186–2193.